P2.13 SPECTRAL DENSITIES OF POLARIMETRIC VARIABLES FOR RETREIVING WINDS AND DETERMINING SCATTERER TYPES

Svetlana Bachmann* and Dusan Zrnic
Cooperative Institute for Mesoscale Meteorological Studies, University of Oklahoma and
NOAA/OAR National Severe Storm Laboratory, Norman, Oklahoma

1. INTRODUCTION

Analyses of polarimetric spectral densities obtained with the S-band research radar located in Norman, Oklahoma are presented.

The weather radar moments and polarimetric variables computed with standard techniques (Doviak and Zrnic 1984) are biased if two or more types of scatterers with different polarimetric properties are present in the radar resolution volume. Generally, returns from the resolution volume are characterized by a set of numbers (moments and polarimetric variables). We derive polarimetric variables from the spectral densities, and therefore for each polarimetric variable instead of a mean value we obtain its distribution in the velocity space. Such distributions provide a unique way for observing multiple processes in resolution volumes and understanding the values of the resulting polarimetric averages.

We examine range-averaged polarimetric distributions as a function of azimuth and time for a clear air case which occurred on September 7, 2004. These data capture the evolution of the transition process between diurnal and nocturnal scatterers. We construct an ensemble of the two-dimensional histograms to assess the occurrence of scatterers moving at a certain velocity and exhibiting certain polarimetric properties. Therefore the statistics of the contributing scatterer types is exposed. The echo types are recognized and a novel approach for velocity azimuth display (VAD) analysis from the histograms is presented. The mean flows of different scatterer types are deduced from the clusters with large occurrences and similar polarimetric properties in the 2-dimensional histograms of polarimetric density and velocity. We obtain marginal distributions for two dominant types of diurnal and two dominant types of nocturnal scatterers that yield significant new insights into the composite VADs and corresponding PPIs.

Presented technique is capable to assess the degree of contamination in a PPI. For two or more sinusoids in a composite VAD standard techniques for moments and polarimetric variable estimation should be replaced with techniques using judicious spectral analyses followed by the appropriate recognition and filtering schemes.

* *Corresponding author address*: Svetlana Bachmann, University of Oklahoma, CIMMS, Norman, OK 73072;

e-mail: svetlana.bachmann@noaa.gov

2. DATA COLLECTION AND ANALYSES

Time-series data were collected with the NOAA NSSL research radar (KOUN) on September 7, 2004. Fair weather and a light N-NW wind were reported on this day; these were good conditions for bird migration. Six cases of echoes collected at the top of each hour from 6 pm (11 UT) to 11 pm local time (4 UT, September 8, 2004) are presented. We use local time notation because it allows a natural association of the progression of the evening with the observed changes.

The radar was in dual polarization mode simultaneously transmitting and receiving waves of horizontal and vertical polarization. The antenna scanned 360° sectors at 0.5° elevation with a pulse repetition time (PRT) of 780 μs (the unambiguous range R_a and velocity v_a were 117 km and 35 m s^{-1} respectively). The number of samples for spectral analysis was M = 128.

The plan position indicators (PPI) of polarimetric variables computed using standard processing technique (Doviak and Zrnic 1984) are shown in Fig.1 with no censoring whatsoever.

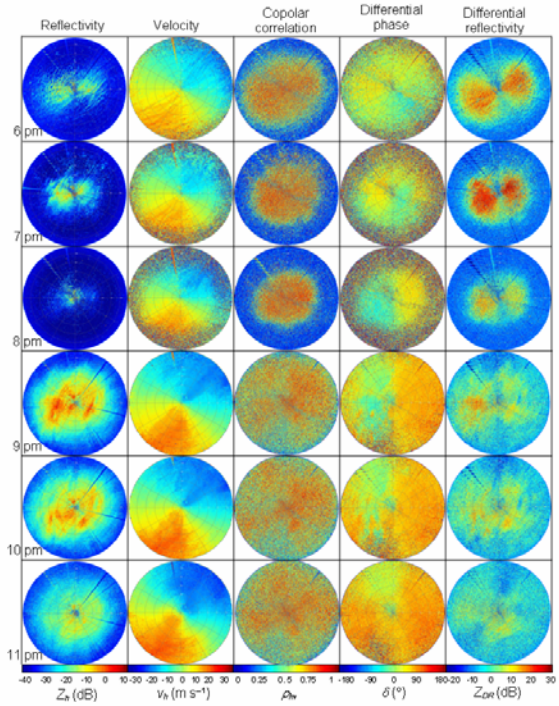

Fig.1. PPIs of clear air and biological scatterers at 0.5° elevation and indicated times on Sept. 7, 2004.

Because clear air echoes are generally weak the standard censoring techniques might result in very sparsely filled radar displays. The portion of the trustworthy echoes can be assessed not from the powers, but rather from the high values of the ρ_{hv}.

The PPIs are expected to show polarimetric properties of the contributing echoes. A biological scatterer has a characteristic shape. A change in the angle between the propagation direction and the axis of scatterer is anticipated to produce a gradual change in the corresponding polarimetric value. The dependence in azimuth is expected to be systematic and to have some symmetry. However, the PPIs display bizarre shapes in the irregular locations. The PPIs indicate that the dominant scatterers at 6 pm descend by 8 pm and get replaced by a different type(s) of scatterers. The symmetry in Z_{DR} PPI is apparent at 6, 7 and 8 pm. The symmetry in PPIs of all polarimetric variables at 8 pm is remarkable. All PPIs display unforeseen values, bizarre shapes and velocities exceeding 25 m s^{-1} at 9, 10 and 11 pm. However, the rawinsonde measured calm winds below 12 m s^{-1} at low altitudes. The disagreement between the atmospheric sounding and radar returns is large. The abnormalities in these cases are attributed to contamination by biological scatterers (Bachmann and Zrnic, 2006). We seek an explanation for the peculiar shapes and unrealistic values of moments and polarimetric variables in the PPIs by examining the polarimetric spectral densities.

3. POLARIMETRIC SPECTRAL DENSITIES

Power spectral density (PSD) is estimated from the time-series data weighted with the von Hann window for each channel (H and V) of the dual polarization weather radar. The noise level is estimated for each range location from the rank order statistics on spectral coefficients. The smallest quarter of the spectral coefficients is averaged to obtain a noise level in the spectrum. The noise levels are estimated for both channels and removed from the corresponding PSD. The spectral densities of differential reflectivity (Z_{DR}) are computed for every H-V pair of spectral coefficients of the PSDs (Kezys et al. 1993, Yanovsky et al. 2005, Bachmann and Zrnic 2006) according to

$$Z_{DR}(k) = 10 \log_{10} (|s_h(k)|^2 / |s_v(k)|^2) + C, \text{ (dB)}, \quad (1)$$

where $s_h(k)$ and $s_v(k)$ are an H-V pair of complex spectral coefficients; C is the calibration constant that accounts for the difference in the system gains of the two channels; k is an ordered number of spectral coefficient that can be transformed to its equivalent radial velocity in the unambiguous velocity interval from $-v_a$ to v_a. The spectral densities of the complex copolar correlation coefficient is estimated from a running 3-point average on $s_h(k)$ and $s_v(k)$ (Bachmann and Zrnic 2006) according to

$$\rho_{hv}(k) = \sum_{m=<k-1>_M}^{<k+1>_M} s_h(m) s_v^*(m) \Big/ \sqrt{\sum_{m=<k-1>_M}^{<k+1>_M} |s_h(m)|^2 \sum_{m=<k-1>_M}^{<k+1>_M} |s_v(m)|^2} . \quad (2)$$

The spectral density of the backscatter differential phase (δ), is computed relative to the system phase

$$\delta(k) = \arg[\rho_{hv}(k)] - \mathit{SystemPhase}. \quad (3)$$

The system phase of the KOUN digital receiver is estimated from the ground clutter reflectivity returns (Zrnic et al. 2005).

4. SPECTRAL DENSITY IN RANGE AND TIME

Example of the polarimetric spectral densities in one radial (azimuth 180°, elevation 0.5°) for the time instances 7, 8, 9, 10, and 11 pm are presented in Fig.2. Color shows the values of S_h, ρ_{hv}, δ, and Z_{DR}. Only densities with ρ_{hv} larger than 0.7 are shown. Doppler Spectrum (Fig.2 S_h) depicts several paths formed by backscattered powers above the background noise. The path at zero velocity shows the residuals from ground clutter filtering. The ground clutter was removed in the frequency domain with a notch-and-interpolate filter. Another path at about 10 m s^{-1} is due to the insects carried by the wind while the path at about 20 m s^{-1} is due to migrating birds. The spectrum width (width of the path) changes as the evening progresses. The spectral width of about 7 m s^{-1} at 6 pm narrows to 5 m s^{-1} at 8 pm; increases again to more than 20 m s^{-1} by 9 pm and stays wide from 9 pm to 11 pm.

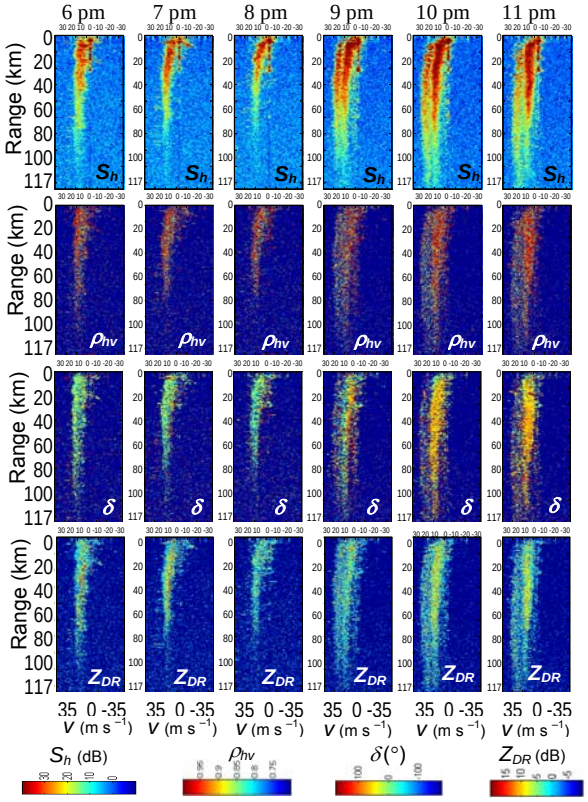

Fig.2. Polarimetric spectral densities in one radial (azimuth 180°, elevation 0.5°) at the top of each hour from 6 pm until 11 pm (local time).

We explain these changes by the gradual transformation of the content within the resolution volume from diurnal to nocturnal biological scatterers. Active flying diurnal insects contribute to a wider spectrum at 6 pm. These insects descend prior to the sunset, causing the narrowing of the spectral width at 7 pm and 8 pm. Nocturnal insects and birds rise after sunset when the main flow of nocturnal bird migration starts. Both birds and insects use the wind to increase distances they travel overnight. Birds, being larger and faster flyers, can adjust their heading so that often it does not coincide with the wind direction. Radar detects a combination of echoes from birds and insects (passive and/or active). The velocities of scatterers are superimposed, which causes a dramatic increase in the spectral width at 9 pm. As long as migration continues the spectrum stays wide (10 pm, 11 pm, etc.). The velocities and directions estimated from such echoes using standard techniques are wrong and represent neither wind nor bird migration velocity. The spectrum width exceeding 20-m s^{-1} clearly shows two paths at the velocities of approximately 10 m s^{-1} and 20 m s^{-1}. If the scatterers in the paths have different polarimetric properties the paths can be discriminated and both velocities can be extracted. In Fig.2 they have. One path (10 m s^{-1} at 180° radial) includes echoes mostly from insects. Another path (20 m s^{-1} at 180° radial) contains purely bird echoes. The values of ρ_{hv}, δ, and Z_{DR} in the insect/wind path are different from the corresponding values in the bird path (Zrnic and Ryzhkov 1998, Bachmann and Zrnic 2006). The signal power in the paths decreases with range and dissipates. However, the range where the peak power is 20 dB above the noise level extends to 70 km (Fig.2 S_h). The polarimetric values in the paths do not exhibit significant changes in range (Fig.2 ρ_{hv}, δ, Z_{DR}). The velocities associated with the paths increase at close ranges (from 0 to 10 km) and then appear stable. Hence, we choose spectral densities between ranges 20 and 70 km to assess the statistics of the echo content in a radial in a 2-dimensional histogram.

5. HISTOGRAM OF RANGE-AVERAGED SPECTRAL DENSITY IN AZIMUTH AND TIME

Fig.3a, b and c show 2-dimensional histograms of Z_{DR}, ρ_{hv} and δ respectively. Each histogram illustrates the prevalence of scatterers with certain polarimetric values in a radial as a function of radial velocity. The 30° degree increments on azimuths from 30° to 360° and one hour time increments from 6 to 11 pm are shown for the sake of space. Gray shade represents the occurrences, with a larger occurrence depicted by a darker color. Azimuthal and time dependences of the polarimetric spectral densities can be observed from this ensemble. The distributions of scatterers' polarimetric properties form bands (ρ_{hv}, Z_{DR}), squiggles (Z_{DR}) and clusters (ρ_{hv}, or δ).

The scatterers with a narrow spread of velocities and high ρ_{hv} values dominate at 7 and 8 pm.

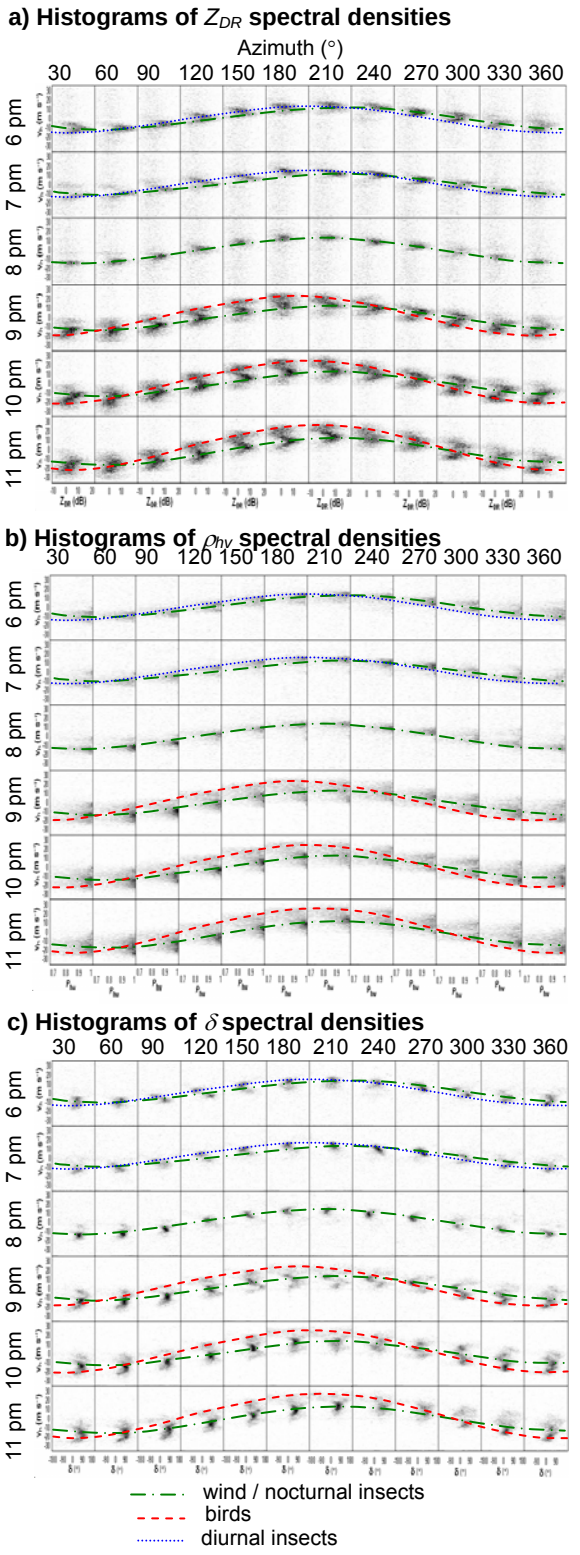

Fig. 3. Ensemble of histograms of a) Z_{DR}, b) ρ_{hv} and c) δ. Each histogram shows echoes within ranges from 20 and 80 km. The VAD sinusoids of contributing scatterers are indicated.

The velocity distribution is slightly broader at 6 pm and much broader at 9, 10 and 11 pm. There is a pattern with two features in the ρ_{hv} distribution in azimuths 30° through 210° at 10 pm and 11 pm. First is the concentrated cluster of scatterers (blobs) with ρ_{hv} in the interval 0.9 to 1 and smaller velocity values. Second is the elongated distribution of scatterers with ρ_{hv} in the interval 0.7 to 1 and larger velocity values. We submit that the blobs with high ρ_{hv} values are caused by the wind-carried small insects.

The simultaneous (ρ_{hv}, δ, and Z_{DR}) VAD analyses allows to locate three sinusoids. The VAD sinusoids of wind, insects and birds are shown with dash-dotted, dotted, and dashed lines respectively.

The high concentration of scatterers with similar phase and velocity forms blobs which are most distinct at 8 pm. At earlier times these are smeared in both velocity and phase, sometimes forming two focus points (blobs). The VAD sinusoids clarify the cause of such a division by grouping the wind blobs with a dash-dotted line and the additional blobs by a dotted line. A small velocity difference (about 3 m s^{-1}) and a directional shift (about 30°) obscure the two scatterer types in the histograms at 6 pm and 7 pm. At later times (9, 10, 11 pm) the wind blobs are surrounded by the irregularly shaped clusters with the apparent dependency in azimuth. The scatterers with high velocities at azimuths 180° through 240° display full range of δ (-180° < δ < 180°) at 9 pm. These are caused by birds. However, the same scatterers at different azimuths occupy only a shorter interval of δ making it difficult to identify the scatterer type.

At the first glance the Z_{DR} histograms (Fig.3a) display complicated squiggles. However, the maximum Z_{DR} value in all averages represents the insects. In the presented case it appears that the dominant nocturnal insects are passive wind tracers and represent the wind (dash-dotted sinusoid). All additional scatterers contribute to bias the wind velocity (dashed and dotted lines). Furthermore, the difference in the heading of the scatterer types (maximum in the sinusoids) complicates the situation and cause asymmetry on the composite PPIs. The polarimetric values depend not only on azimuth but also on the directional shift between the scatterers mean flows.

We obtain objective wind VAD (wind velocities) by connecting appropriate clusters in the ensemble of histograms. The clusters with similar differential phase are used at 6 and 7 pm. The blobs from either histogram can be used at 8 pm. The clusters with the maximum Z_{DR} values are used at 9, 10, and 11 pm.

7. CONCLUSIONS

We have demonstrated that unreasonable values of polarimetric variables computed with standard techniques are often a result of a mixture of different types of scatterers. The distributions of polarimetric variables in velocity provide a unique way for observing multiple processes in each resolution volume and understanding the values of the resulting polarimetric averages. Presented technique can be used for quality assessment of the spectral moments and polarimetric variables. If there is one sinusoid in the VAD there is one type of dominant scatterers and the moments in PPIs can be trusted. Otherwise, the moment show biased estimates and should be recalculated using more sophisticated (spectral) techniques.

Acknowledgements

For the first author funding was provided by NOAA/Office of Oceanic and Atmospheric Research under NOAA-University of Oklahoma Cooperative Agreement #NA17RJ1227, U.S. Department of Commerce.

8. REFERENCE

Bachmann S. M., and D. S. Zrnić, 2006: Spectral Density of polarimetric variables separates biological scatterers in the VAD display. Submitted to the *Jour. Atmos. Oceanic Technology*

Doviak R. J., and D. S. Zrnić, 1984: Doppler Radar and Weather Observations. Academic Press, 458 pp.

Kezys V., E. Torlaschi, and S. Haykin, 1993: Potential capabilities of coherent dual polarization X-band radar. Preprints, 26th Int. Conf. on Radar Meteorology, Norman, OK, Amer. Meteor. Soc., 106-108.

Yanovsky, F.J., H.W.J. Russchenberg, and C.M.H. Unal, 2005: Retrieval of information about turbulence in rain by using Doppler-polarimetric Radar. IEEE Trans. Microw. Theory Tech., **53,** 444- 450

Zrnić D. S, and A. V. Ryzhkov, 1998: Observation of Insects and Birds with Polarimetric Radar. IEEE Trans. Geosci. Remote Sens., 36, 661-668.

Zrnić D. S., V. M. Melnikov, and A.V. Ryzhkov, 2005: Correlation coefficients between horizontally and vertically polarized returns from ground clutter. Submitted to the *Jour. Atmos. Oceanic Technology*